Electronic Supplementary Material (ESI) for Journal of Materials Chemistry A.
This journal is © The Royal Society of Chemistry 2020

Switchable Molecular Sieving of Capping Metal Organic Framework Membrane

Shuai Zhang, Bo Gui, Teng Ben*[a] and Shilun Qiu

[a] *Department of Chemistry, University of Jilin, No. 2699 Qianjin Street, Changchun, Jilin Province, 130012, P. R. China. E-mail: tben@jlu.edu.cn*

[b] *Key Laboratory of Biomedical Polymers of Ministry of Education, College of Chemistry and Molecular Sciences, No. 299 Bayi Road, Wuhan, Hubei Province, 430072, P. R. China*

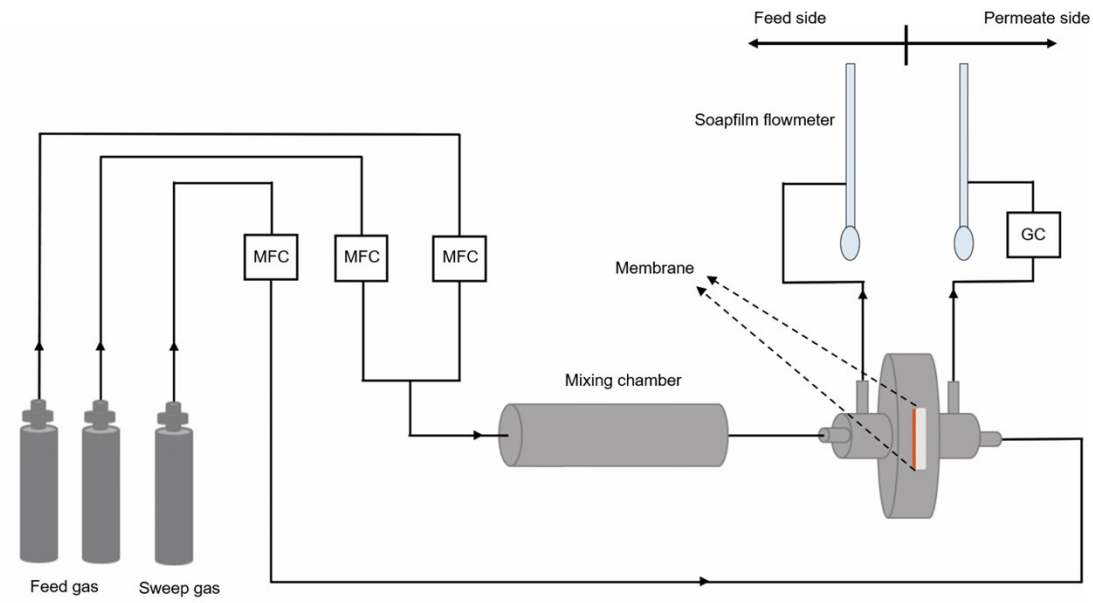

Scheme S1. Schematic illustration of gas separation set-up (MFC: Mass flowmeter controller; GC: Gas chromatograph).

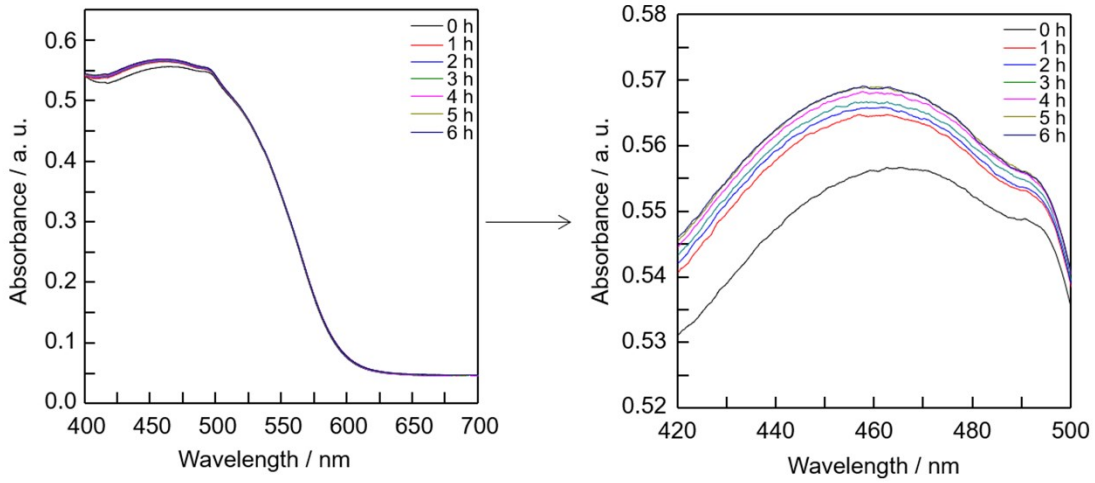

Figure S1. UV-visible spectra of UiO-68-azo after exposure to UV light (365 nm) for different time.

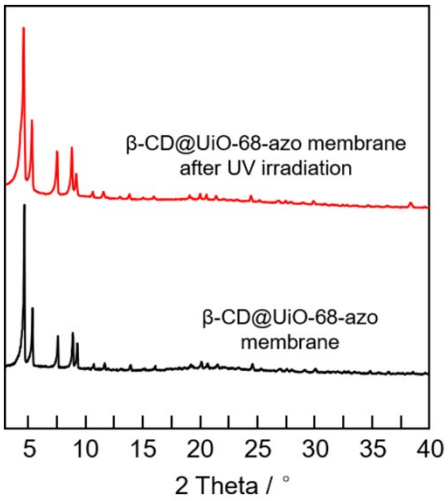

Figure S2. The XRD patterns of UiO-68-azo before (black) and after (red) UV irradiation.

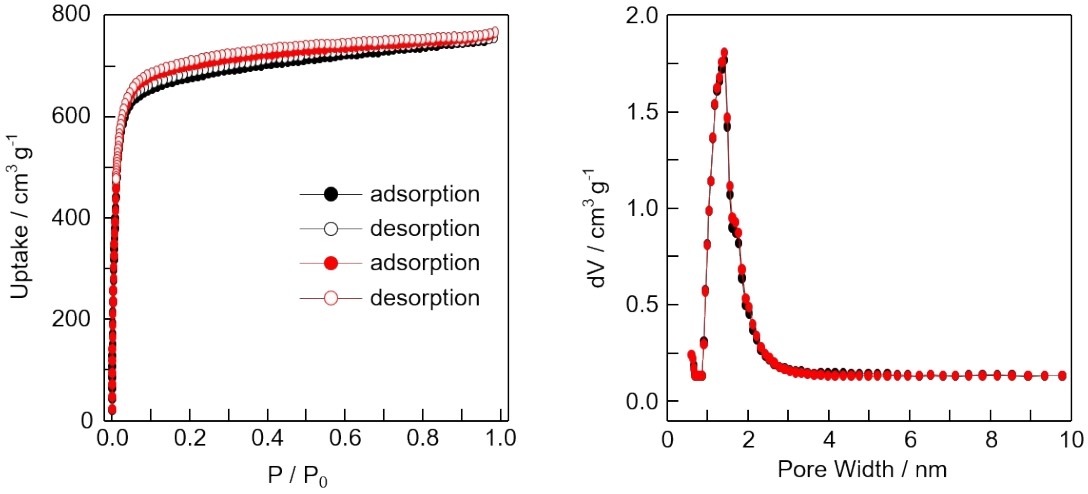

Figure S3. The N_2 sorption isotherm and pore size distribution of UiO-68-azo (black) and UiO-68-azo after UV irradiation (red). The BET surface area and pore size are 2629 $m^2 g^{-1}$, 2717 $m^2 g^{-1}$ and 1.41 nm, 1.41nm respectively.

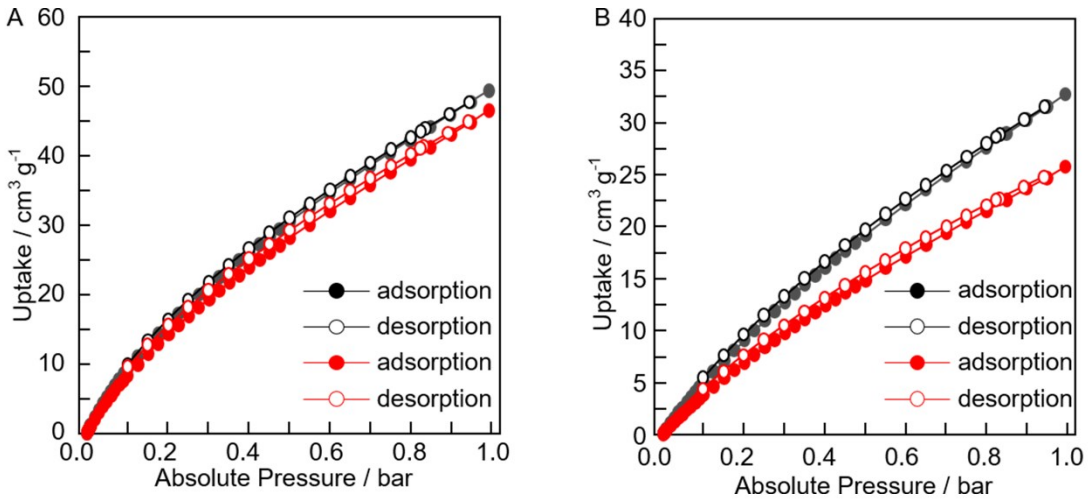

Figure S4. The CO_2 sorption isotherms of UiO-68-azo (black) and UiO-68-azo after UV irradiation (red) at A) 273 K and B) 298 K.

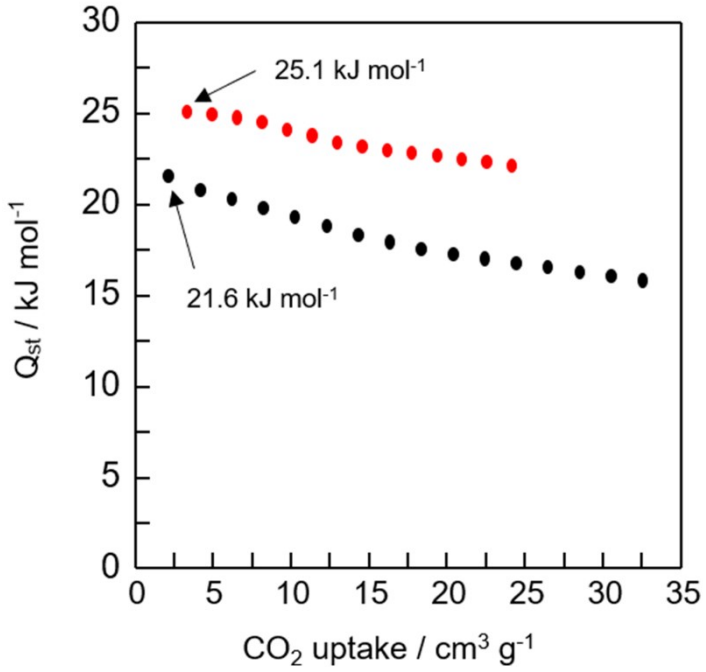

Figure S5. The isosteric enthalpy Q_{st} of CO_2 for UiO-68-azo (black) and UiO-68-azo after UV irradiation (red). The Q_{st} are 21.6 kJ mol^{-1} and 25.1 kJ mol^{-1} respectively.

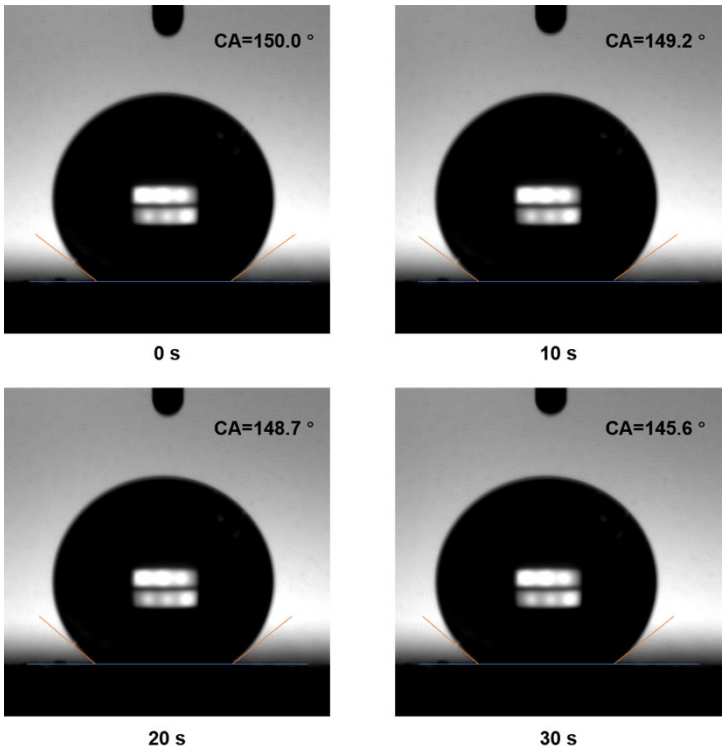

Figure S6. Droplet profiles with inserted static contact angle (CA) value (upper-right corner) on the UiO-68-azo membrane surface at different measuring time.

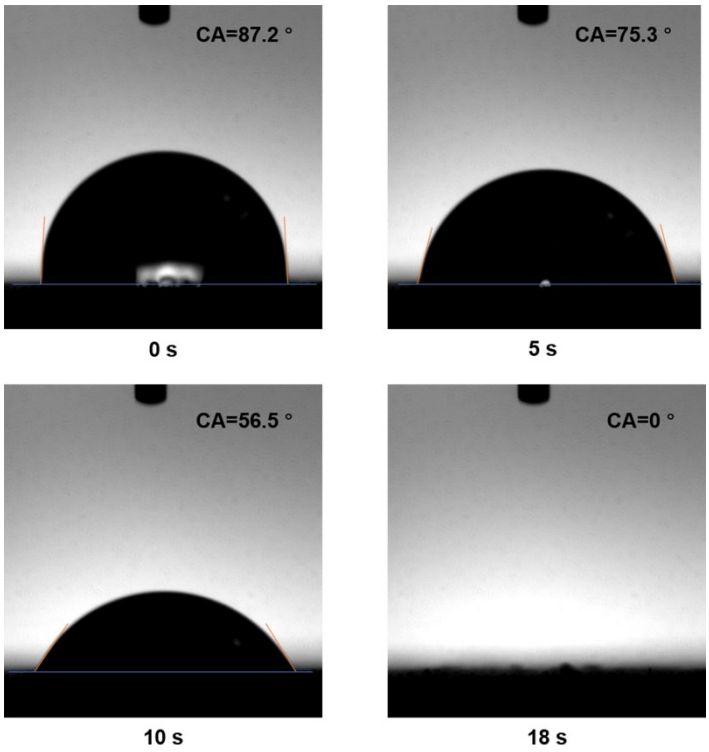

Figure S7. Droplet profiles with inserted static contact angle (CA) value (upper-right corner) on the β-CD@UiO-68-azo membrane surface at different measuring time.

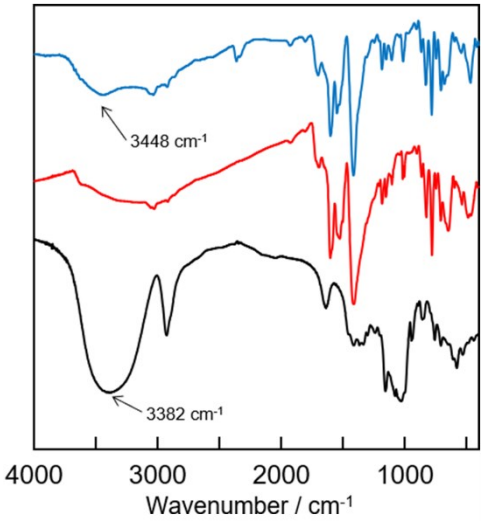

Figure S8. Anhydrous FTIR spectrums of β-CD (black), UiO-68-azo (red) and β-CD@UiO-68-azo (blue).

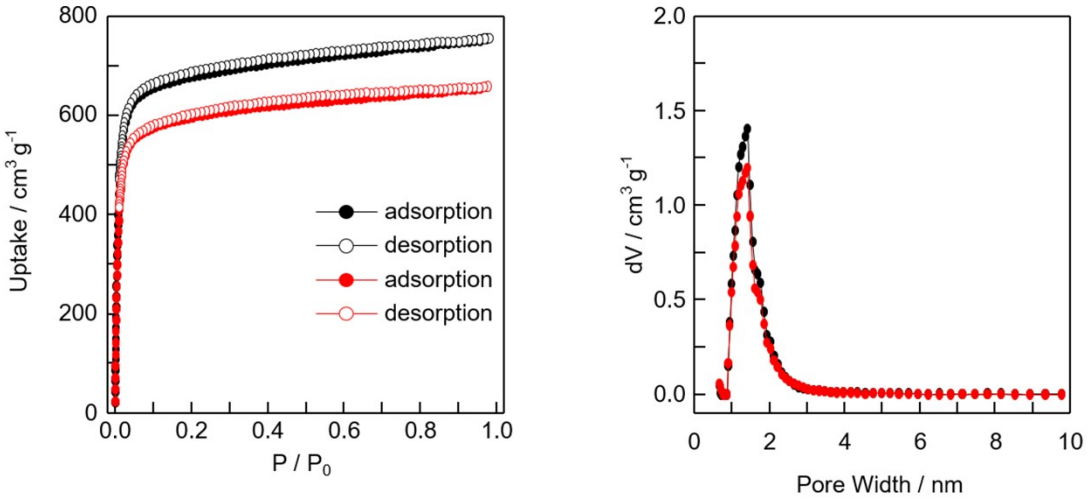

Figure S9. The N_2 sorption isotherm and pore size distribution of UiO-68-azo (black) and β-CD@UiO-68-azo (red). The BET surface area and pore size are 2629 m^2 g^{-1}, 2311 m^2 g^{-1} and 1.41 nm, 1.41 nm respectively.

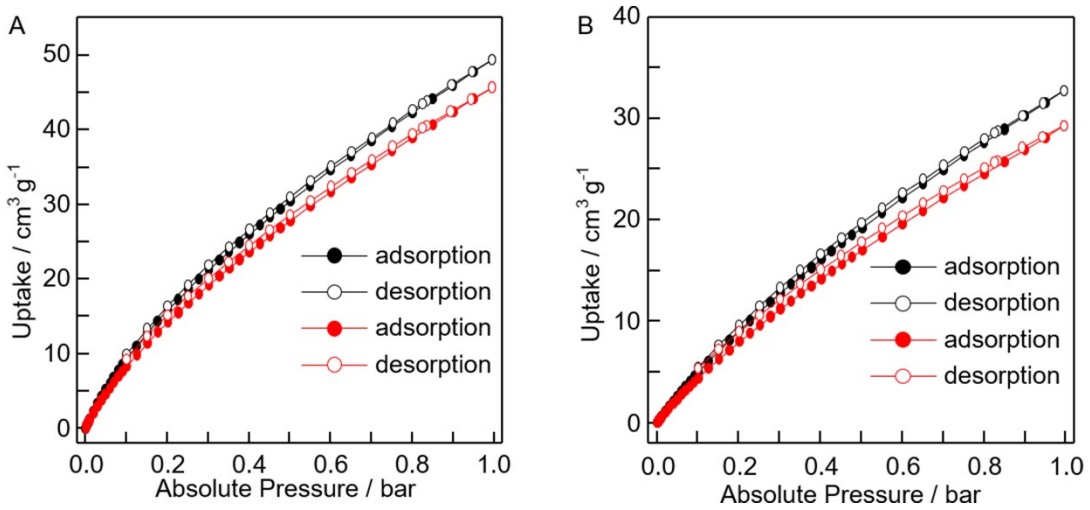

Figure S10. The CO_2 sorption isotherms of UiO-68-azo (black) and β-CD@UiO-68-azo (red) at A) 273 K and B) 298 K.

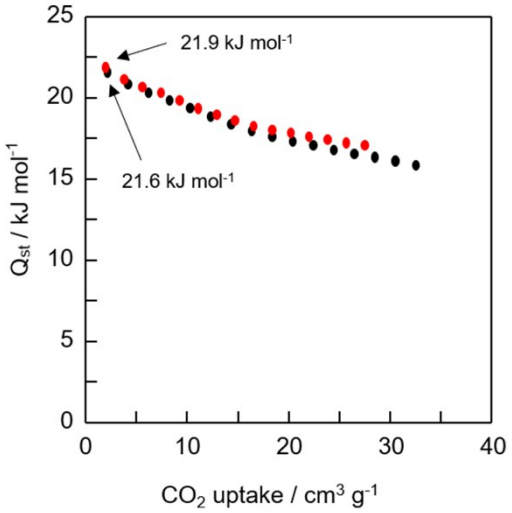

Figure S11. The isosteric enthalpy Q_{st} of CO_2 for UiO-68-azo (black) and β-CD@UiO-68-azo (red). The Q_{st} are 21.6 kJ mol^{-1} and 21.9 kJ mol^{-1} respectively.

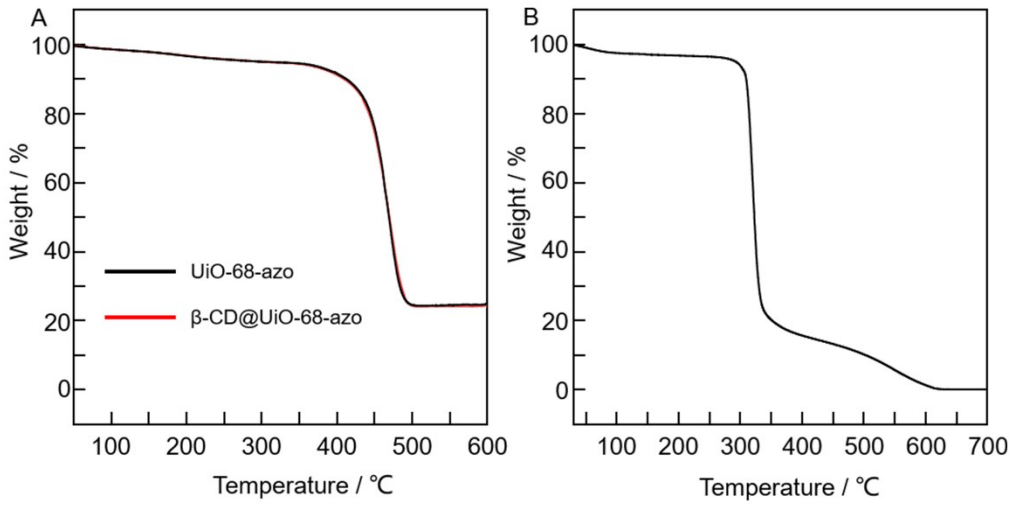

Figure S12. TGA curves of A) UiO-68-azo (black), β-CD@UiO-68-azo (red) and B) β-CD at atmosphere.

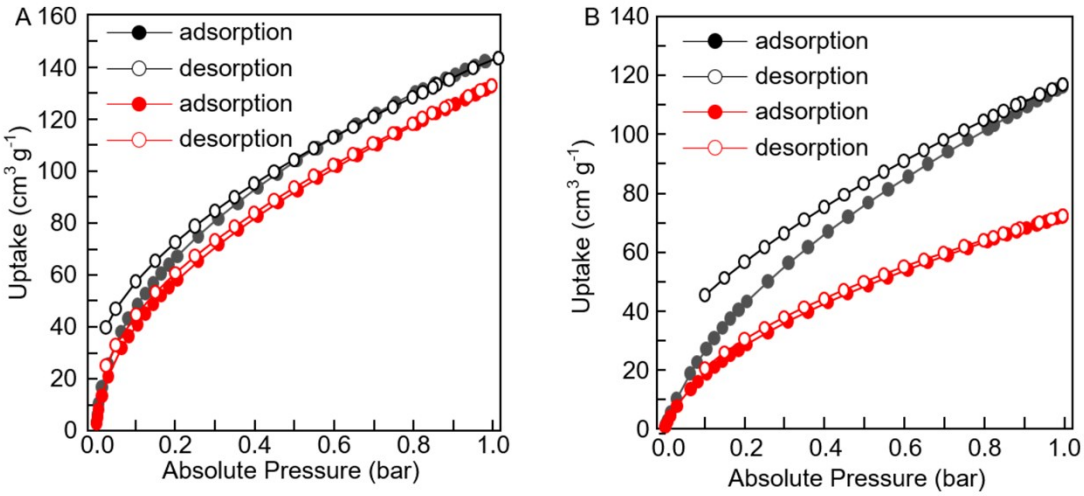

Figure S13. The H_2 adsorption of UiO-68-azo (black) and β-CD@UiO-68-azo (red) at A) 77 K and B) 87 K.

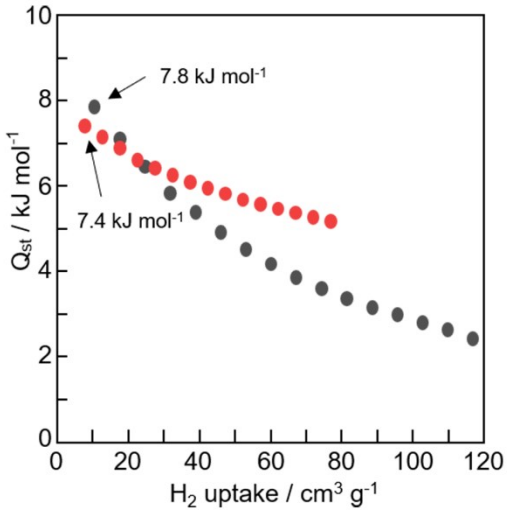

Figure S14. The H_2 Qst of UiO-68-azo (black) and β-CD@UiO-68-azo (red). The Qst are 7.8 kJ $mol^{-1}$and 7.4 kJ mol^{-1} respectively.

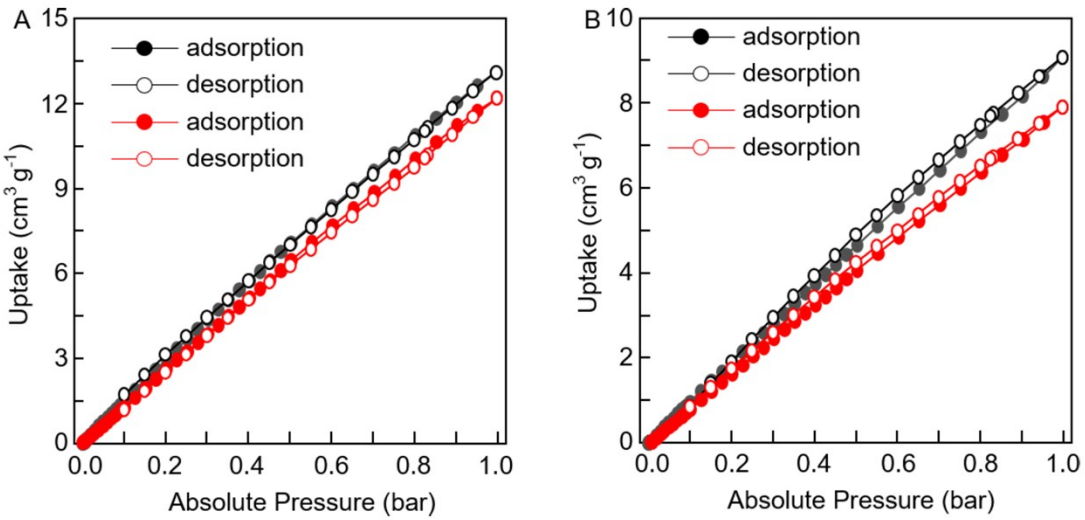

Figure S15. The CH_4 adsorption of UiO-68-azo (black) and β-CD@UiO-68-azo (red) at A) 77 K and B) 87 K.

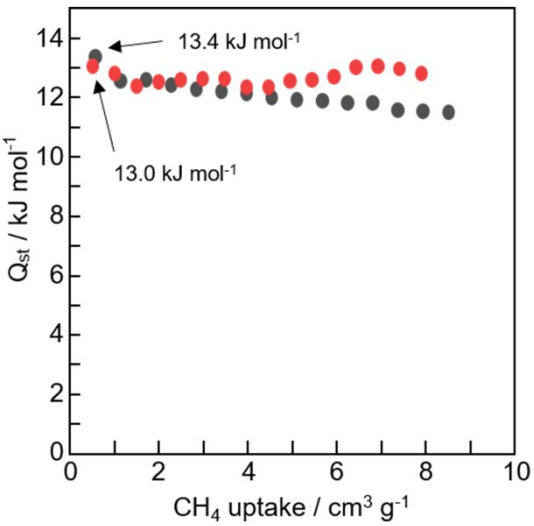

Figure S16. The CH_4 Qst of UiO-68-azo (black) and β-CD@UiO-68-azo (red). The Qst are 13.4 kJ $mol^{-1}$and 13.0 kJ mol^{-1} respectively.

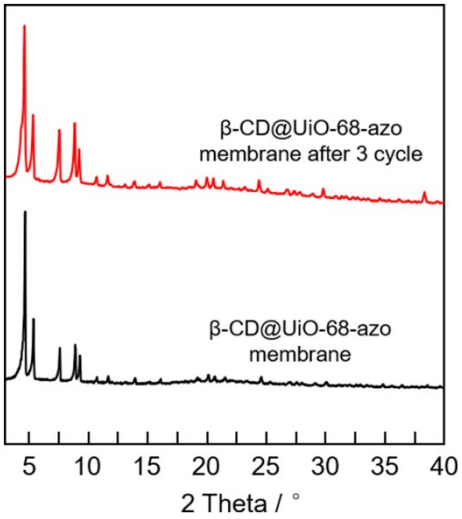

Figure S17. The XRD patterns of UiO-68-azo membrane (black) and β-CD@UiO-68-azo membrane after 3 cycle of desorption/adsorption of β-CD (red).

Table S1. H_2/CO_2 mixture gas separation performances of the UiO-68-azo membrane before and after UV irradiation at 1 bar and room temperature with 1:1 binary mixture.

		UiO-68-azo membrane			UiO-68-azo membrane after UV irradiation		
Membrane	KC[a]	P (i)[b]	P (j)[b]	SF[c]	P (i)[b]	P (j)[b]	SF[c]
1		131520	13152	14.9	121702	9447	17.9
2		132076	12596	15.4	121702	9261	18.0
3	4.7	145783	18523	13.5	144301	17968	14.6
4		130038	12967	16.5	121331	9076	18.6
5		143560	16671	16.1	142449	16486	17.2

[a.] Knudsen constant. [b.] Permeability in Barrer. [c.] Separation factor.

Table S2. Mixture gas separation performances of the UiO-68-azo membrane and β-CD@UiO-68-azo membrane at 1 bar and room temperature with 1:1 binary mixture. (Membrane 1)

		UiO-68-azo membrane			β-CD@UiO-68-azo membrane		
$Gas_{i/j}$	KC[a]	P (i)[b]	P (j)[b]	SF[c]	P (i)[b]	P (j)[b]	SF[c]
H_2/CO_2	4.7	130779	12781	15.0	107253	2778	46.6
H_2/N_2	3.7	116145	14819	10.8	103919	5186	23.9
H_2/CH_4	2.8	107253	23154	9.7	110958	9632	13.1

[a.] Knudsen constant. [b.] Permeability in Barrer. [c.] Separation factor.

Table S3. Mixture gas separation performances of the UiO-68-azo membrane and β-CD@UiO-68-azo membrane at 1 bar and room temperature with 1:1 binary mixture. (Membrane 2)

		UiO-68-azo membrane			β-CD@UiO-68-azo membrane		
$Gas_{i/j}$	KC[a]	P (i)[b]	P (j)[b]	SF[c]	P (i)[b]	P (j)[b]	SF[c]
H_2/CO_2	4.7	130038	12781	16.5	107809	2558	48.9
H_2/N_2	3.7	119479	17227	9.3	102993	4797	21.9
H_2/CH_4	2.8	130223	22414	7.8	110958	8314	12.9

[a.] Knudsen constant. [b.] Permeability in Barrer. [c.] Separation factor.

Table S4. H_2/CO_2 Mixture gas separation performances of β-CD@UiO-68-azo membrane at 1 bar and different temperature (from 303 K to 323 K) with 1:1 binary mixture.

		β-CD@UiO-68-azo membrane		
Temperature / °C	KC[a]	P (i)[b]	P (j)[b]	SF[c]
30		102596	2957	44.8
40	4.7	108388	3455	41.1
50		118592	4964	32.5

[a.] Knudsen constant. [b.] Permeability in Barrer. [c.] Separation factor.

Table S5. H_2/CO_2 Mixture gas separation performances of β-CD@UiO-68-azo membrane at room temperature and different pressure (feed gas pressure from 1bar to 1.4bar) with 1:1 binary mixture.

		β-CD@UiO-68-azo membrane		
Pressure / bar	KC[a]	P (i)[b]	P (j)[b]	SF[c]
1		99237	2686	47.3
1.1	4.7	97865	2864	42.4
1.4		80132	4931	20.3

[a.] Knudsen constant. [b.] Permeability in Barrer. [c.] Separation factor.